

Developing force-deformation characteristics of brick masonry spandrels in historic buildings



K. Beyer

Ecole Polytechnique Fédérale de Lausanne (EPFL), Switzerland

A. Dazio

EUCENTRE, Pavia, Italy

SUMMARY:

When subjected to seismic loading, unreinforced masonry buildings may form kinematic mechanisms, which can be broadly characterised into two types: i) weak pier-strong spandrel, and ii) strong pier-weak spandrel. Type i) represents a soft storey mechanism, where most of the damage is concentrated in the piers of one storey. In Type ii) mechanisms, damage largely concentrates in the spandrels and is therefore typically distributed over the height of the building. Frequently, a combination of Type i) and ii) mechanisms occurs. If buildings develop mechanisms comprising significant damage to the spandrels, the prediction of their seismic behaviour requires knowledge on the nonlinear force-deformation behaviour of the spandrels. While such relationships are available for piers, they are currently lacking for spandrels. This paper contributes to the definition of force-deformation relationships for masonry spandrels by introducing a piecewise linear approximation whose characteristic points are determined for four spandrels that were tested experimentally. Furthermore, it introduces simple mechanical models for estimating the peak and residual strength of spandrels.

Keywords: Brick masonry, spandrel elements, force-deformation relationship, shear strength, deformation capacity.

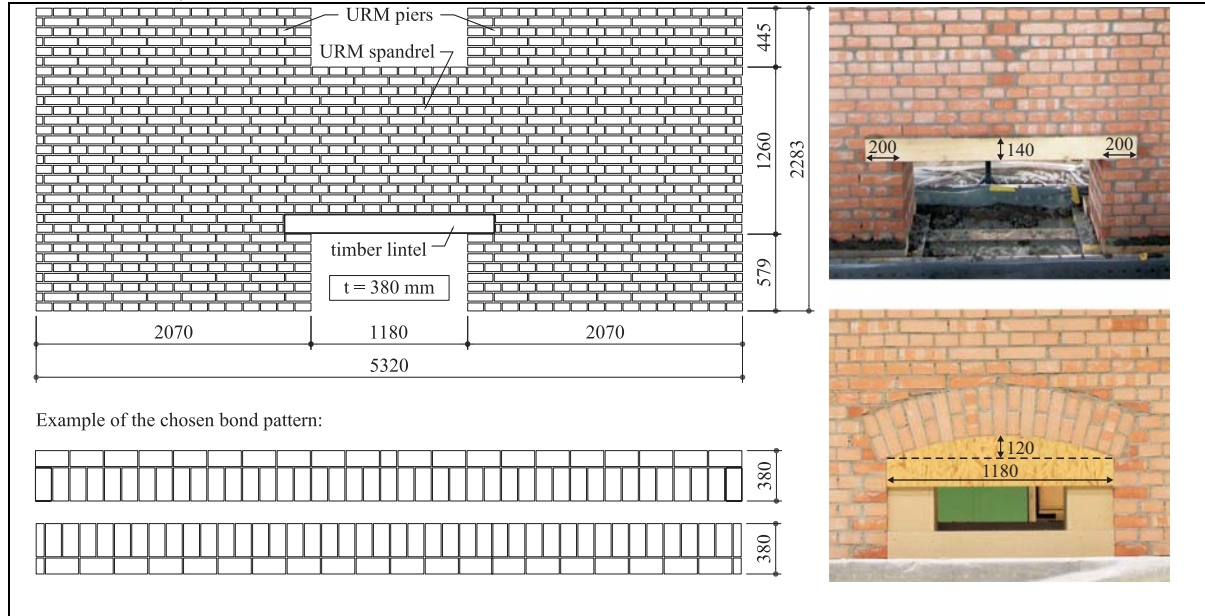
1. INTRODUCTION

The main structural elements of unreinforced masonry (URM) buildings are piers and spandrels. While there is certainly still considerable need for research concerning the force and drift capacities of URM piers, the lack of knowledge related to URM spandrels is disproportionately larger. A large number of tests on different types of URM piers with different geometries was conducted in the past by different researchers. The results of these tests allowed validating and calibrating mechanical models for the pier strength. Moreover, by means of statistical analysis, the experimental results allowed also deriving estimates for parameters for which mechanical models are still not well established, e.g. for the effective elastic stiffness and drift capacities of piers.

Mechanical and empirical models for masonry spandrel elements are considerably less advanced or even not available since experimental evidence on the force-deformation behaviour of URM spandrels was missing for a long time. Only very recently, tests on spandrel elements were conducted by different research groups which will allow developing such models. This paper is a contribution to the definition of a piecewise linear force-deformation relationship for masonry spandrels in a building subjected to seismic loading. The paper begins with a short summary of the scope of the test programme on masonry spandrels that forms the basis of the work. Next is the description of a piecewise force-deformation relationship for spandrels and the evaluation of the characteristic points from the experimental data gained from the quasi-static tests. Finally, mechanical models for estimating the peak and residual strength of masonry spandrels are summarised.

known from the shear failure of masonry piers. The flexural failure mode is observed for small axial spandrel forces while the shear failure mode is observed for large axial spandrel forces. In a real building, the axial force in the spandrel is caused by horizontal steel ties and/or adjacent piers that partially restrain the axial elongation of the spandrel when the spandrel cracks. In the test, this restraining effect was simulated by the horizontal steel ties.

Table 1. Loading scheme, spandrel type and details of the axial load application for the four test units (Beyer and Dazio, 2012).



Test Unit	Loading	Spandrel type	Axial stress in piers	Axial force in spandrel
TUA	Cyclic	Timber lintel	0.33 MPa	Constant first 80 kN, then 40 kN
TUB	Cyclic	Timber lintel	0.33 MPa	Variable, plain bar with low axial stiffness
TUC	Cyclic	Masonry arch	0.43 MPa	Constant 80kN
TUD	Cyclic	Masonry arch	0.43 MPa	Variable, plain bar with high axial stiffness

3. FORCE-DEFORMATION RELATIONSHIPS FOR MASONRY SPANDRELS

3.1. Characteristics of the force-deformation relationship of masonry spandrels

A spandrel is a horizontal structural element in a perforated masonry wall. When such a masonry wall is subjected to in-plane horizontal loading, the spandrel is subjected to a deformation mode as shown in Figure 2a. The corresponding sectional forces acting on the spandrel are shown in Figure 3a. In a large perforated masonry wall with regular openings and pier dimensions, the spandrel displacement and the spandrel rotation can be computed as (Figure 2b, Milani *et al.*, 2009):

$$\Delta_{sp} = \theta_{pier} (l_{pier} + l_{sp}) \quad (1)$$

$$\theta_{sp} = \theta_{pier} \frac{(l_{pier} + l_{sp})}{l_{sp}} \quad (2)$$

From the quasi-static tests, the envelopes of the cyclic force-deformation relationships were determined and all four tests showed envelopes with a shape similar to the schematic force-

deformation relationship for a masonry spandrel shown in Figure 3b. The characteristic points of this force-deformation relationship are described hereafter; a more detailed discussion can be found in Beyer (2012). The figure shows on the positive vertical axis the spandrel shear force as a function of spandrel rotation θ_{sp} . As outlined in Section 2, the spandrel behaviour is strongly dependent on the axial compression force P_{sp} applied to the spandrel. For this reason, Figure 3b shows on the negative vertical axis the axial compression force in the spandrel as a function of the spandrel rotation θ_{sp} . At the onset of the test, an axial force P_{sp0} was applied to the spandrel. As outlined in Section 2, for TUA and TUC the axial force was constant during the entire test, i.e., the axial force P_{sp} was independent of the imposed rotation θ_{sp} . For TUB and TUD, however, the axial force in the spandrel was dependent on the spandrel rotation θ_{sp} . As soon as the spandrel cracked, it tended to elongate and the stress in the horizontal tie rods which partially restrained the axial elongation spandrel increased as the spandrel grew in length and therefore applied an axial force on the spandrel which increased with increasing spandrel deformation.

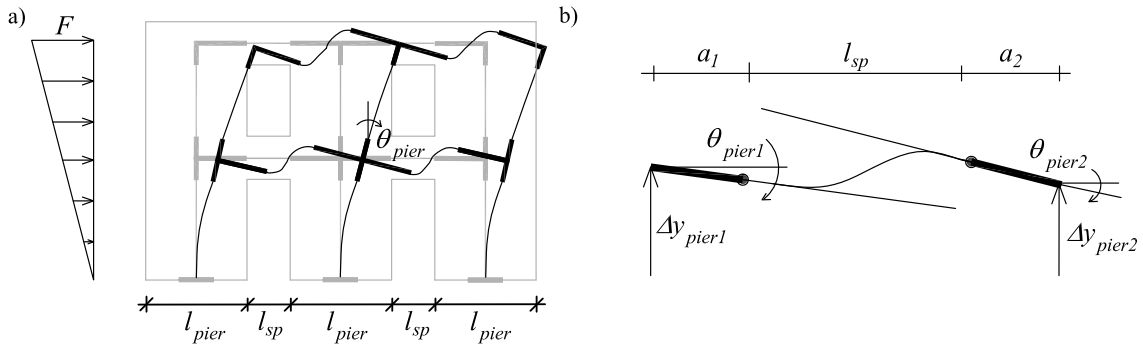


Figure 2. (a) Deformation of a perforated masonry wall modelled using an equivalent frame model subjected to horizontal in-plane loading. (b) Deformation of the spandrel element in the equivalent frame when the deformations of the pier left and right to the spandrel are equal.

At the beginning of the test, the shear force increased almost linearly up to V_{cr} when the first cracks in the spandrel formed (Figure 3b). The stiffness then reduced until the peak shear strength V_p was reached. At this point, the number and size of cracks increased and the spandrel strength dropped to a residual strength. The residual strength was strongly dependent on the axial force P_{sp} and varied therefore if the axial force P_{sp} varied (TUB and TUD). The onset of material degradation led eventually to a reduced stiffness and strength of the spandrel and finally to its failure.

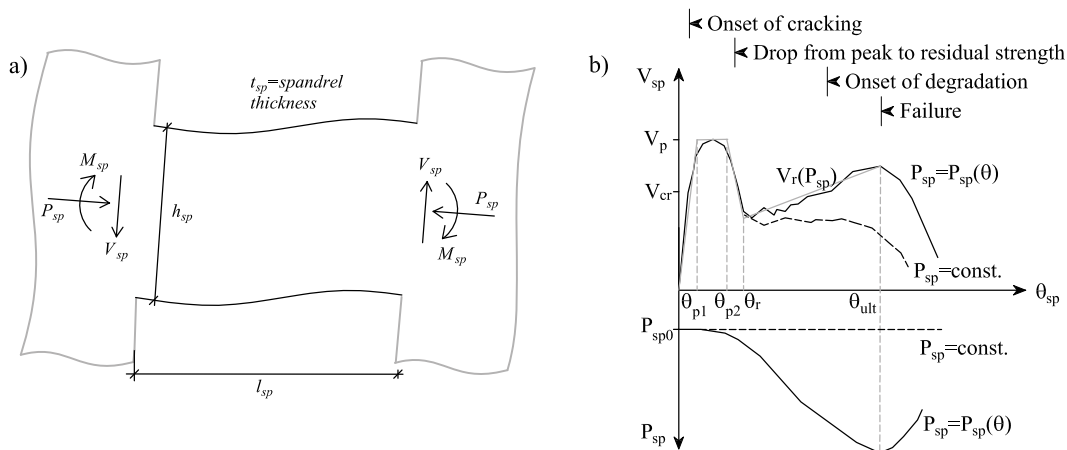


Figure 3. Deformation of a spandrel subjected to horizontal in-plane loading (a). Characteristic force-deformation relationship of a masonry spandrel subjected to such a deformation (b) (Beyer, 2012).

3.2 Evaluation of quasi-static cyclic tests on masonry spandrels

The objective of this section is to approximate the experimentally determined force-deformation envelopes of test units TUA to TUD by a piecewise linear relationship as shown in Figure 3b. The

approximation was based on the following definitions:

- Initial branch representing the effective elastic stiffness of the spandrel: The effective stiffness was determined as the best-fit line passing through the origin and the points before the plateau strength was reached.
- Peak strength V_p : If the plateau characterising the peak strength of the spandrel was rather short, V_p was defined as the maximum value of this plateau. If the plateau was rather long, it was defined as the mean strength of the values making up the plateau.
- Limit rotation θ_{p1} : The spandrel rotation θ_{p1} was defined as the point of intersection of the initial branch and the plateau.
- Limit rotation θ_{p2} : If the plateau characterising the peak strength of the spandrel was rather short, θ_{p2} was defined as the rotation at peak strength V_p . If the plateau was rather long, it was defined as the rotation before the strong drop in force was observed.
- Limit rotation θ_r : The rotation θ_r marks the onset of the branch of the force-deformation curve characterising the residual strength of the spandrel.
- Ultimate rotation θ_{ult} : The ultimate rotation is defined as the maximum rotation of the cycle for which a strong degradation was not yet observed. The strong degradation is typically associated with the onset of failure of a lintel support (TUA, TUB) or the fracturing of bricks within the masonry arch due to high compressive and shear stresses (TUC, TUD).

The here proposed definition of ultimate rotation differs from the generally applied definition by Park (1988). Park defines the ultimate deformation capacity as the rotation at which the strength of the structural element has reduced to 80% of its peak value. This definition of the deformation capacity has been applied widely to reinforced concrete structural elements and also to unreinforced masonry piers (e.g., Frumento *et al.*, 2009). For masonry spandrels, however, this definition would lead to rather small deformation capacities as the drop in strength after attaining the peak strength typically exceeds 20% V_p . Hence, applying the definition by Park, the ultimate rotation capacity would correspond to a value between θ_{p2} and θ_r and the often rather stable force-deformation behaviour of the spandrel for rotations larger than θ_r would be neglected in the assessment of the structure. For example, if Park's definition is applied to the four spandrels tested, the ultimate rotation capacity of all spandrel, except TUB, would be between θ_{p2} and θ_r and vary between 0.28 and 0.39, which corresponds to pier rotations between 0.18 and 0.26 (see Eqn. (2)). Hence, if the deformation capacity of the spandrels was defined according to Park, the spandrels would reach their rotation capacity before the piers reached theirs. The spandrel should therefore be neglected in the assessment of the ultimate behaviour of the building – an approach which seems overly conservative if the rather stable force-deformation behaviour of the spandrel for rotations larger than θ_r is considered.

The force-deformation envelopes of the four spandrels tested were approximated using the method outlined above and the characteristic points of the resulting piecewise linear envelopes are summarised in Table 2 and visualised in Figure 4. Apart from the spandrel rotations, Table 2 gives the corresponding pier rotations as values in brackets. The results show that the peak strength values were attained for rotations θ_{p2} up to 0.3% and 0.5%, which corresponds to pier rotations of 0.1% to 0.2%. The ultimate rotation θ_{ult} of the spandrels varied between 1.7% and 4.1%, which corresponds to pier rotations of 0.6% to 1.5%.

3.3 Comparison of the rotation capacities of masonry spandrels to the drift capacities of masonry piers

The European design code Eurocode 8 (CEN, 2005) suggests for piers failing in shear a drift limit of 0.4% and for piers failing in flexure a drift limit of 0.8% H_0/D , where H_0/D is the shear ratio. These values represent the damage state “significant damage”. For the damage state “near collapse”, Eurocode 8 proposes to multiply these drift limits by 4/3. The ultimate rotation capacity θ_{ult} of the spandrels as defined in Section 3.2 corresponds to the limit state “significant damage”.

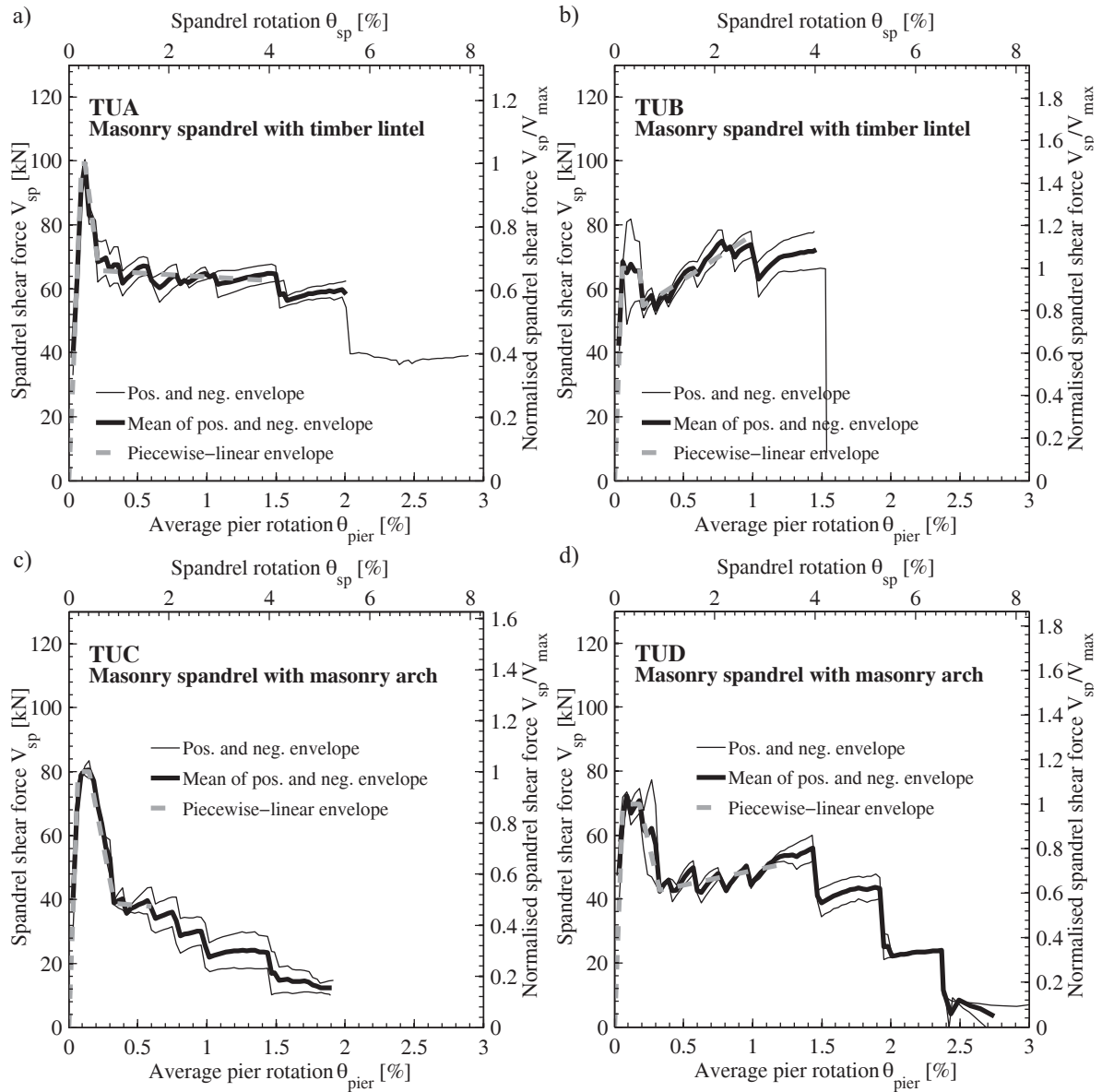


Figure 4. Force-deformation envelopes for masonry spandrels: Experimental results and their piecewise linear approximation.

The force-deformation envelopes in Figure 4 show that the maximum rotation attained during testing is at least $4/3$ times the deformation capacity θ_{ult} . The definition of the ultimate spandrel rotation suggested in Section 3.2 therefore satisfies the relationship defined in Eurocode 8 between the deformation capacities at the two limit states “significant damage” and “near collapse”. For the chosen geometry of piers and spandrels, the spandrel rotations need to be multiplied by $l_{sp}/(l_{sp}+l_{pier})=0.36$ to derive equivalent pier rotations. When comparing the spandrel rotation capacities to those of a pier failing in shear (Eurocode 8: $\theta_{pier}=0.4\%$), the ultimate rotation capacity is larger than the drift capacity of the pier. Hence, if the piers develop a shear mechanism, the ultimate resistance of the structure can be computed considering the residual strength of the spandrels. If the piers were failing in flexure, they would have an estimated deformation capacity of $0.8\% H_0/D$. Assuming a shear ratio equal to unity, the deformation capacity of all tested spandrels, with the exception of TUC, would be again larger than the drift capacity of the piers. Figure 5 shows for a regular perforated wall the required rotation capacity of the spandrels which ensures that the spandrels fail after the piers. The rotation capacity is expressed as a function of the ratio of the spandrel length to the pier length and the pier rotation capacity. The figure also indicates the rotation capacities of the four tested spandrels. For the tested configuration the length ratio was $l_{sp}/l_{pier}=0.57$.

Table 2. Characteristic values of the piecewise linear force-deformation envelopes for TUA-TUD.

	θ_{p1} [%]	$V(\theta_{p1})/V_p$ [-]	θ_{p2} [%]	$V(\theta_{p2})/V_p$ [-]	θ_r [%]	$V(\theta_r)/V_p$ [-]	θ_{ult} [%]	$V(\theta_{ult})/V_p$ [-]
TUA	0.26 ¹⁾ (0.10) ²⁾	1	0.33 (0.12)	1	0.60 (0.22)	0.66	4.13 (1.50)	0.63
TUB	0.15 (0.06)	1	0.50 (0.18)	1	0.57 (0.21)	0.82	2.72 (0.99)	1.15
TUC	0.19 (0.07)	1	0.41 (0.15)	1	0.91 (0.33)	0.48	1.65 (0.60)	0.47
TUD	0.16 (0.06)	1	0.50 (0.18)	1	0.90 (0.33)	0.61	3.47 (1.26)	0.74

¹⁾ Spandrel rotation θ_{sp}

²⁾ Equivalent rotation of pier $\theta_{pier} = \theta_{sp} \frac{l_{sp}}{l_{sp}+l_{pier}} = 0.36 \cdot \theta_{sp}$

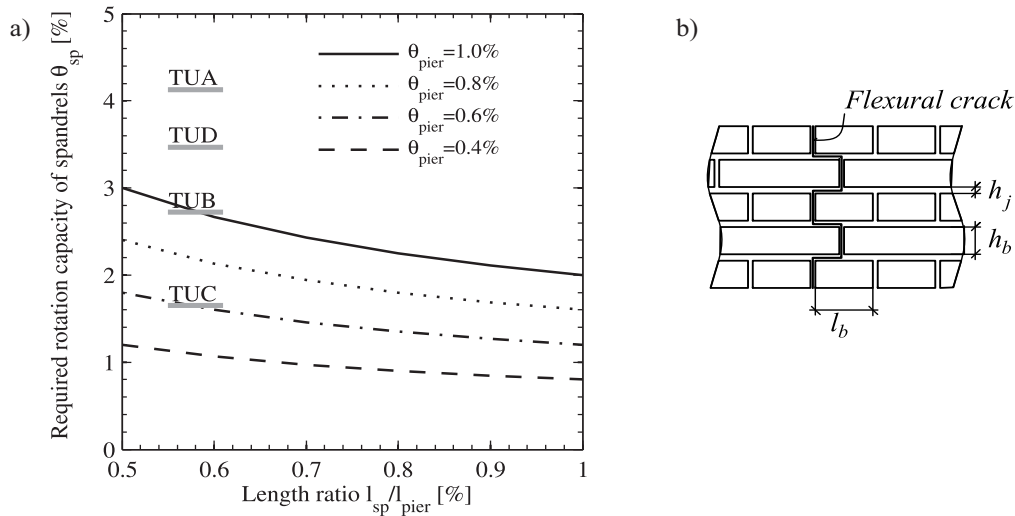


Figure 5. Required rotation capacity of the spandrels to avoid premature failure of the spandrels (a). Geometry of the brick layout (b).

4. MECHANICAL MODELS FOR ESTIMATING THE PEAK AND RESIDUAL STRENGTH OF MASONRY SPANDRELS

Apart from estimates of limit rotations, estimates of the peak and residual strength of masonry spandrels are required in order to construct the force-deformation relationship of masonry spandrels. Existing strength models were reviewed in Beyer and Mangalathu (2012) and modified ones, which can account also for the contribution of a timber lintel or a shallow masonry arch, proposed in Beyer (2012). Table 3 summarises the equations for estimating the peak and residual strength of a masonry spandrel developing either a flexural or a shear mechanism if the contribution of a timber lintel or a masonry arch is neglected. The proposed equations are based on simple mechanical models. They were applied to TUA – TUD and the experimental results were estimated well (Beyer, 2012).

5. CONCLUSIONS

Equivalent frame models of perforated masonry walls require the definition of force-deformation relationships for pier and spandrel elements. While such relationships have already been established for piers, they are yet to be accurately defined for spandrels. This paper makes a contribution towards the definition of a force-deformation relationship for masonry spandrels by (i) defining a piecewise linear force-deformation envelope, (ii) evaluating the response of tested spandrel elements with respect to the limit rotations which characterise the piecewise linear envelope and by (iii) proposing equations for estimating the peak and residual strength of masonry spandrels.

Table 3. Summary of strength equations for masonry spandrels neglecting the contribution of a timber lintel or a masonry arch

Flexural mode	Shear mode
Onset of cracking: Not considered	Onset of cracking: $V_{cr,s} = \frac{2}{3} c_p h_{sp} t_{sp}$ Assumption: The stress on the bed joints at midspan is approximately zero.
Peak strength: $V_{p,fl} = (f_t + p_{sp}) \frac{h_{sp}^2 t_{sp}}{3 l_{sp}}$ $f_t = (0.5 \mu_p \sigma_{pier} + c_p) \frac{l_b}{2(h_b + h_j)} + \frac{c_p}{2 \mu_p}$	Peak strength (cracks through joints): $V_{p,s1} = \frac{2}{3} (c_p + \mu_p p_{sp}) \cdot h_{sp} t_{sp}$ Peak strength (cracks through bricks): $V_{p,s2} = h_{sp} t_{sp} \frac{f_{bt}'}{2.3(I + \alpha_v)} \sqrt{1 + \frac{p_{sp}}{f_{bt}'}}$
Residual strength: $V_{r,fl} = \frac{P_{sp} h_{sp}}{l_{sp}} \left(1 - \frac{P_{sp}}{0.85 f_{hm}} \right)$	Residual strength: $V = 0$

Where:

- μ_p and c_p are the friction coefficient and cohesion, respectively, which are describing the joint peak strength by means of a Mohr-Coulomb relationship.
- σ_{pier} is the mean axial stress in the piers, p_{sp} is the mean axial stress in the spandrel.
- h_{sp} , t_{sp} , l_{sp} are related to the geometry of the spandrel and are defined in Figure 3a.
- h_b , h_j , l_b are related to the geometry of the brick layout and are defined in Figure 5b.
- f_{hm} , f_{bt}' are the horizontal compressive strength and the diagonal tensile strength of the spandrel, respectively.
- α_v is the shear ratio of the spandrel. As an approximation it can be assumed that the spandrel is subjected to double bending: $\alpha_v = l_{sp}/2h_{sp}$.

The analysis of the tested spandrel elements showed that for most geometries the spandrel deformation capacity is larger than the equivalent pier deformation capacity that is defined in Eurocode 8 (CEN, 2005) if the residual strength of the masonry spandrel is accounted for. As the drop from peak to residual strength typically exceeds 20% of the peak strength, the ultimate deformation capacity should be linked to the onset of material degradation rather than to a residual strength of 80% of the peak strength. The latter definition is commonly applied to RC structural elements and unreinforced masonry piers but in the case of masonry spandrels it would lead to rather small ultimate deformations which neglect the significant deformation capacity associated with the often rather stable residual strength mechanism.

REFERENCES

- Beyer, K. (2012). Peak and residual strengths of brick masonry spandrels. *Engineering Structures*: 41, 533-547.
- Beyer, K., Dazio, A. (2012). Quasi-static cyclic tests on masonry spandrels. *Earthquake Spectra*, in press.
- Beyer, K., Mangalathu, S. (2012). Review of strength models for masonry spandrels. Submitted to the *Bulletin of Earthquake Engineering*.
- CEN (2005). Eurocode 8: Design of structures for earthquake resistance – Part 3: General rules, seismic actions and rules for buildings. EN 1998-3. European Committee for Standardisation, Brussels, Belgium.
- Frumento, S., Magenes, G., Morandi, P., Calvi, G.M. (2009). Interpretation of experimental shear tests on clay brick masonry walls and evaluation of q-factors for seismic design. IUSS Press, Pavia, Italy.
- Milani, G., Beyer, K., Dazio, A. (2009). Upper bound limit analysis of meso-mechanical spandrel models for the pushover analysis of 2D masonry frames. *Engineering Structures*: 31(11), 2696-2710.
- Park, R. (1988). Ductility evaluation from laboratory and analytical testing. Proceedings of the Ninth World Conference on Earthquake Engineering, Tokyo-Kyoto, Japan, VIII-605-616.